Strategies for Dose Reduction and Improvement of Image Quality in Chest CT

Narinder S. Paul

Abstract

The last two decades have witnessed a dramatic escalation in the utilization of computed tomography (CT) for diagnostic purposes, and there has been a corresponding increase in patient and physician concern regarding the potential for long-term carcinogenesis. Therefore it is essential to embrace the ALARA principle in which radiation exposures are maintained "as low as reasonably achievable" and progressive improvements in CT design and software algorithms have facilitated significant reductions in radiation exposure while maintaining diagnostic image quality. This chapter is not meant to provide an exhaustive review of all these advances but instead will focus on the advances that are applicable to a wider scope of clinical applications in adult chest CT. The material will be discussed under the following sections: appropriateness guidelines, x-ray tube assembly, patient-related factors, and x-ray detector and post-processing algorithms.

1 Introduction

The last two decades have witnessed a dramatic escalation in the utilization of computed tomography (CT) for diagnostic purposes (Brenner and Hall 2007; Hricak et al. 2011), and there has been a corresponding increase in patient and physician concern regarding the potential for long-term carcinogenesis (Einstein et al. 2007). Therefore it is essential to embrace the ALARA principle in which radiation exposures are maintained "as low as reasonably achievable" and progressive improvements in CT design and software algorithms have facilitated significant reductions in radiation exposure while maintaining diagnostic image quality. This chapter is not meant to provide an exhaustive review of all these advances but instead will focus on the advances that are applicable to a wider scope of clinical applications in adult chest CT. The material will be discussed under the following sections: appropriateness guidelines, x-ray tube assembly,

N.S. Paul
Department of Medical Imagining, Toronto General Hospital, University Ave, University of Toronto, Toronto, ON, Canada
e-mail: Narinder.Paul@uhn.ca

U.J. Schoepf, F.G. Meinel (eds.), *Multidetector-Row CT of the Thorax*, Medical Radiology,
DOI 10.1007/978-3-319-30355-0_2

patient-related factors, and x-ray detector and post-processing algorithms.

2 Appropriateness Guidelines

Clinical practice is conventionally based on experience and the best clinical opinion; however, there is increased focus on appropriateness guidelines supported by evidence-based practice. Organizations such as the American College of Radiology (www.acr.org) and the Royal College of Radiologists (www.rcr.ac.uk) provide access to a wide scope of appropriateness guidelines. More chest-focused imaging tasks are addressed through the use of specific "rules" based on clinical algorithms such as the Wells score (Wells et al. 1998) and the modified Wells score (Wells et al. 2001) for pulmonary embolism. These guidelines should be used to inform local practice in utilization of imaging resources, especially modalities that issue ionizing radiation.

3 X-Ray Tube Assembly

The x-ray tube consists of a negatively charged cathode aligned with a positively charged anode placed within a glass vacuum tube. Mobile electrons are generated in the cathode filament by the x-ray tube current and accelerated to the anode by the x-ray tube potential. Photoelectric and Compton's interactions in the anode produce x-ray photons that are transmitted through the object (patient) and registered on the detector elements. The width of the x-ray beam is controlled by the aperture of the x-ray beam collimator.

The x-ray tube current determines the number of x-ray photons that are produced, and the x-ray tube potential determines the energy of these photons. The combination of the x-ray tube current and tube potential determines the x-ray exposure to the patient and, depending on the radiation sensitivity of the irradiated tissues, the effective dose to the patient.

Initial strategies at radiation dose reduction focused on reducing the x-ray tube current as the tube current has a linear relationship with radiation exposure and there is a predictable increase in image noise with decrease in the tube current. However, more recent approaches have targeted reductions in x-ray tube potential (Fanous et al. 2012) due to the almost exponential relationship between x-ray tube potential and radiation dose. Consequently, a decrease in x-ray tube potential results in a relatively large change in image noise and image quality, as assessed by the contrast-to-noise ratio. It is important to reiterate that reductions in x-ray tube current do not fundamentally change the energy spectrum of the x-ray beam, merely the amount of x-ray photons generated at each energy level. Alteration of the x-ray tube potential, however, does affect the maximum energy level of the x-ray beam and the transmission of x-rays through the patient. Therefore, there needs to be careful matching of the x-ray tube potential setting to the x-ray absorption characteristics of the patient.

Early attempts to optimize the x-ray exposure parameters to the patient body habitus resulted in bodyweight-based prioritization of x-ray tube potential, followed by using body mass index (Bendaoud et al. 2011) and then by using anthropomorphic measurements of chest dimensions (Rogalla et al. 2010). As the largest constituent organ in the thorax is the lung tissue, with minimum x-ray absorption from the normal lungs, the surrounding chest wall tissues play an important role in determining the absorption of x-ray photons and therefore in image quality (Paul et al. 2011). Therefore, the closest approximation of required x-ray exposure parameters and patient body habitus is achieved through assessment of x-ray absorption at specific anatomic levels (Odedra et al. 2014). This approach facilitates minimization of x-ray exposure parameters while maintaining diagnostic image quality (Newton et al. 2011). Modern CT scanners assess the x-ray absorption profile of the patient's thorax from the scout projections that are acquired to plan the study. Once the absorption profile has been assessed, the system will automatically prioritize the lowest x-ray tube potential for the patient and for the selected protocol; the x-ray tube current will automatically be adjusted to ensure a constant image quality at every anatomical level as

described later. The CT dose index (CTDI) is a measure of the radiation dose per unit of tissue.

Targeting a low x-ray tube potential (70–80 kVp) is of benefit in children and small adults due to the lower x-ray absorption profile. A lower x-ray tube potential (80–100 kVp) is also beneficial in larger patients if the target of interest is enhanced by intravascular injection of iodinated contrast material (CM), as the increased efficiency of x-ray photons to generate signal increases as the x-ray tube potential decreases due to increase in the photoelectric effect and approximation of the set x-ray tube potential to the "K edge" of iodine (Nakayama et al. 2005; Murakami et al. 2010). Therefore, for CT studies that focus on the thoracic aorta or the pulmonary arteries, for an equivalent CTDI, a CT study performed using a lower x-ray tube potential will have an ~30% increase in measured signal from the enhanced structures (Fanous et al. 2012). This facilitates the use of lower x-ray tube potential settings in these examinations. As diagnostic utility of CT is related to the signal-to-noise ratio (SNR) in an image, if the target structures have increased signal from the enhanced CT protocol, diagnostic utility can be maintained at a higher image noise and therefore a lower x-ray tube current setting.

Many body tissues exhibit an increase in x-ray absorption with a decrease in x-ray photons; at the x-ray potentials used in diagnostic imaging, this change is relatively small for the cortical bone and for body fluids but is substantially larger for injected iodinated CM (Godoy et al. 2009). Therefore, for CT scans enhanced with intravascular iodinated CM, if image data is acquired using low and high settings of x-ray tube potential (kV), post-processing of image data can result in several different images: a low- and a high-kV image, a weighted average image, a virtual non-contrast image, a virtual contrast image (iodine predominant), and a bone subtraction image (Godoy et al. 2009). The weighted average CT image provides a comparable image to a conventional CT acquisition; if there are technical difficulties causing suboptimal contrast enhancement or increased image noise, then the increased iodine signal in the low-kV image can maintain the diagnostic utility of a study. The virtual non-contrast study can be used to obviate the need for a prior non-contrast study (thus saving radiation dose). The iodine predominant study can be used to display the distribution of iodine (blood) in an organ and has been used to demonstrate pulmonary blood distribution in patients with acute and chronic pulmonary embolism (Pontana et al. 2008; Dournes et al. 2014). Dual energy acquisitions can be performed in several ways: using a dual-source CT with each x-ray tube set to different tube potentials, with a single x-ray detector using fast switching between high- and low-kV acquisitions, and with the use of sequential high- and low-kV data acquisitions (Ko et al. 2012; Kaza et al. 2012). Finally, this data could also be provided through modification of the detector system with dual-layer detectors or with detectors sensitive to multiple energy spectra.

Cross-sectional image data is produced as the x-ray tube-detector system rotates around the patient while emitting x-ray projections that transmit through the patient. The radiation exposure from each gantry rotation is a function of the radiation dose per projection and the number of x-ray projections. The radiation exposure can be reduced either by reducing the dose per projection (reduction in x-ray tube potential or current) or by reducing the number of projections. Assuming that the frequency of emitting x-ray projections is constant, an increase or decrease in the speed of the gantry rotation will cause a corresponding increase or decrease in radiation dose. This can be a useful strategy to adjust radiation exposure in situations where the desire is to maintain tissue contrast. For example, in CT pulmonary angiography or aortography, if a low x-ray tube potential is set, but the required x-ray tube current setting exceeds the system capacity for the patient body habitus. In this situation, instead of increasing the kV setting and losing the advantage of extra iodine signal at the lower kV, the tube rotation could be slowed to enable the appropriate tube current flux (tube current x time) to be used and otherwise maintain the exposure settings. A conventional CT image is produced from ~1200 x-ray projections; as the gantry rotation gets faster, there is a corresponding reduction in the number of projections acquired and the subsequent image

quality. This can be offset by increasing the dose per x-ray projection or by using image reconstruction methods other than filtered back projection (FBP). There is considerable interest using a smaller number of x-ray projections to achieve diagnostic image quality at significantly reduced radiation doses by utilizing limited angle data and compressed sensing algorithms in CT (Idky et al. 2006). However, at present these algorithms remain under research evaluation.

The width of the x-ray beam is controlled by the collimator diaphragm. In older CT systems, the position of the diaphragm is fixed during image acquisition; this leads to increased radiation exposure at the beginning and end of helical acquisition due to over-ranging with multidetector CT systems (Schiham et al. 2010). Modern CT systems use dynamic collimator diaphragms that move independently such that the collimator opens asymmetrically at the start and end of a helical acquisition to eliminate the irradiation of tissues outside the range of reconstructed image data.

4 Patient-Related Factors

The CT scout projections acquire data that map the x-ray attenuation profile of the patient in the region of interest. Modern CT systems utilize x-ray scan protocols that maximally optimize x-ray exposure to the x-ray absorption profile of the patient and prioritize the use of the lowest possible x-ray tube potential. As the x-ray absorption profile of the thorax is variable, with increased absorption of x-ray photons at the thoracic inlet and at the thoracoabdominal junction and least absorption at the carina, the x-ray tube current is modulated in the X-Y-Z planes to match this pattern. This dose modulation delivers consistent image quality regardless of patient size or shape and individualized or a personalized CT scan profile (Kalra et al. 2005). However, there are two essential prerequisites; the first is the determination of the level of acceptable image noise, measured as standard deviation in Hounsfield units (HUs), for each scan protocol, and the second is optimal patient positioning. Each CT system is delivered with manufacturer-determined levels of image noise for specific clinical applications. Individual radiology groups may choose more aggressive levels of image noise to drive lower radiation dose levels. The patient needs to be positioned centrally on the CT table, and ideally the patient should be in the isocenter of the CT gantry prior to image acquisition. The use of automatic dose modulation software in patients who are offset by as little as 3 cm from the isocenter of the CT gantry can result in 30 % more radiation dose.

5 X-Ray Detectors and Post-processing Algorithms

Although anti-scatter grids have been used in chest radiography for several decades, the use of an anti-scatter grid has only recently been incorporated into the design of a CT scanner. The mechanism of action is similar to that in chest radiography and is anticipated to be more advantageous in improving image quality in obese patients. Anti-scatter grids are also likely to be more useful in CT systems that have larger detector systems.

Another key determinant of patient radiation dose is related to the efficiency with which the x-ray detector converts incident x-ray photons into light. The transition from gas-filled (e.g., xenon) detectors to solid-state detectors has resulted in ~23 % increase in dose efficiency (Fuchs et al. 2000). There is continued focus on production of low profile-high efficiency detectors and reduction in the background electronic noise that limits contrast resolution for ultralow-dose CT.

Once the x-ray detector has converted the x-ray photons into light, a CT sonogram is formed in the raw data space and translated into the image data space where the trans-axial CT images are formed. Filtered back projection (FBP) has been the cornerstone of CT image processing for decades; the images are of high resolution and require little computation time and resources. However, FBP requires a significant amount of x-ray data in order to produce diagnostic quality images. Therefore, despite the fact that diagnostic quality ultralow-dose (0.2 mSv) lung images can be acquired using FBP, the mediastinum is poorly assessed (Hanna et al. 2014). This interest in low-dose and ultralow-dose CT has,

however, precipitated interest in alternative image post-processing algorithms, in particular iterative reconstruction. Iterative reconstruction (IR) algorithms have been extensively used in modalities such as nuclear medicine in order to produce diagnostic images despite the paucity of image data. However, the prolonged image reconstruction time and the infrastructure cost of the required computational resource were prohibitive for consideration of IR in CT imaging. The recent focus on low-dose imaging combined with a precipitous decrease in cost of computer graphics processing units has made implementation of IR into clinical CT a reality. The first-generation IR algorithms, image-based IR, provided relatively little compromise in image reconstruction times and modest reductions in radiation dose. The subsequent generation of IR algorithms, statistical weight-based algorithms, was a hybrid algorithm located in raw data and image-based domains. The potential reduction in radiation dose was greater, but the image quality compared to conventional FBP remained suboptimal. The latest IR algorithms, model-based IR, are located more in the raw data domain and have improved image quality, but the image reconstruction times remain a challenge. The continued development and refinement of IR algorithms will result in significant improvements in image quality with ultralow-dose thoracic CT (Beister et al. 2012; Yuki et al. 2014; Wang et al. 2014; Spears et al. 2014; Leipsic et al. 2010; Gosling et al. 2010; Di Cesare et al. 2014; Williams et al. 2013; Fujimoto et al. 2013).

Image quality and quantity of x-ray projections

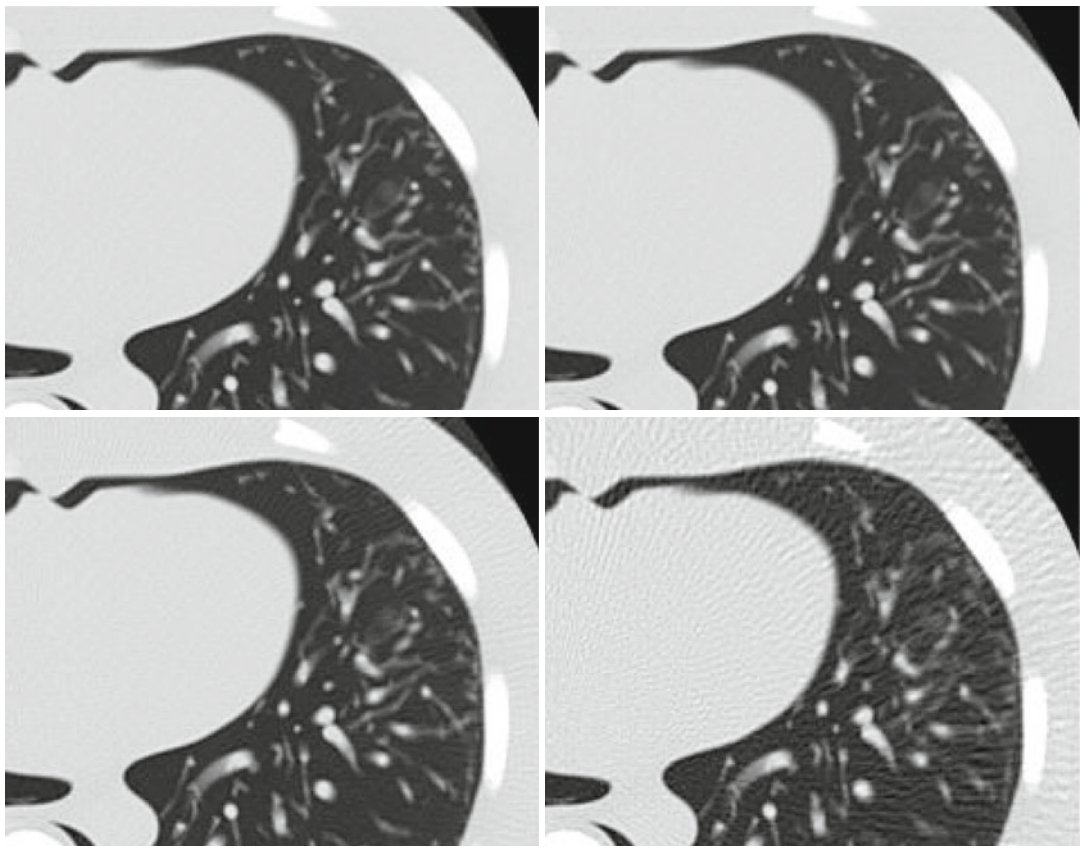

A 10 mm ground glass nodule measuring -800 HU was placed in the left lung of an anthropomorphic chest phantom (Lungman, Kyoto Kagaku) and scanned using 64×0.5 mm detector configuration (AQONE, Toshiba Medical Systems, Japan) with fixed x-ray tube exposure parameters (120 kV, 200 mAs), but the images were reconstructed with a different number of x-ray projections: (**a**) 1200, (**b**) 900, (**c**) 600, and (**d**) 300 projections. Note how artifacts start to appear when the image is reconstructed using 600 projections or less

Ultralow-dose thoracic computed tomography (0.2 mSv)

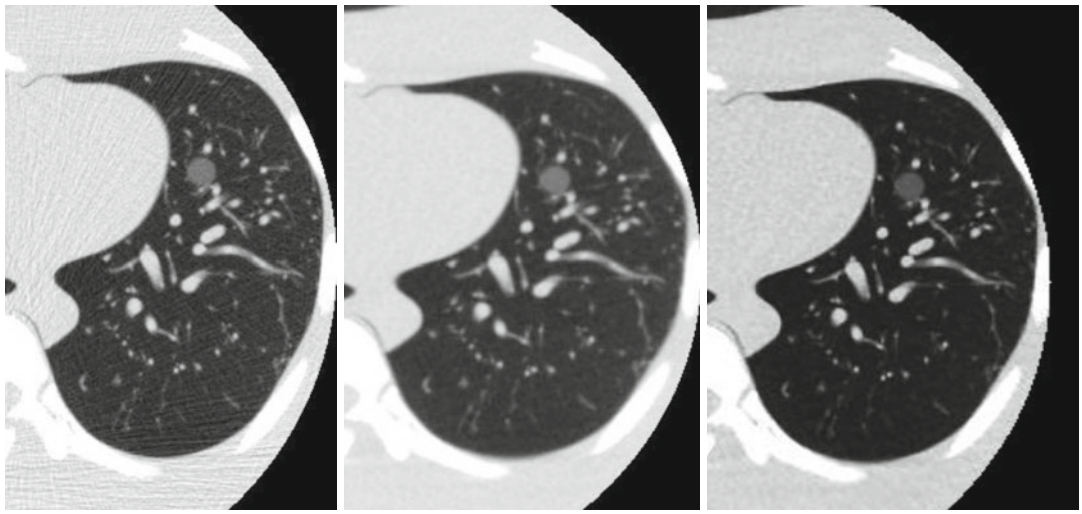

A 10 mm ground glass nodule measuring -800 HU was placed in the left lung of an anthropomorphic chest phantom (Lungman, Kyoto Kagaku) and scanned using 64×0.5 mm detector configuration (AQONE, Toshiba Medical Systems, Japan) with fixed x-ray tube exposure parameters (120 kV, 5 mAs), and the images were reconstructed with filtered back projection, FBP (**a**); third-generation iterative reconstruction, IR (**b**); and model-based IR, MIR (**c**). Note the lack of beam-hardening artifact in the MIR image compared to the FBP image and the improved edge sharpness of the MIR image compared to the IR image

Ultralow-dose thoracic computed tomography (0.2 mSv)

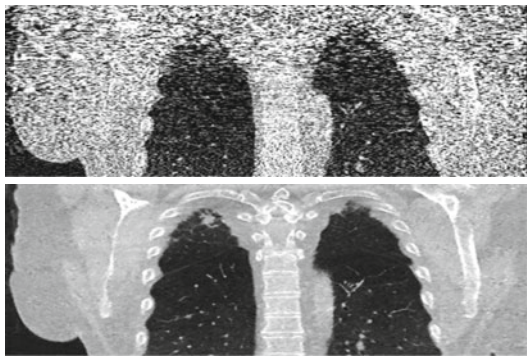

Coronal thin-slice (0.5 mm) CT reconstructions of a patient performed with 64×0.5 mm detector configuration (AQONE, Toshiba Medical Systems, Japan) using fixed x-ray tube exposure parameters (120 kV, 5 mAs), and the images were reconstructed with filtered back projection, FBP (**a**), and model-based IR, MIR (**b**). The 10 mm irregular nodule in the apex of the right lung is clearly visualized on the MIR image but obscured by image noise on the FBP image

6 Summary

Sequential advances in CT scanner design and reconstruction algorithms, adaptation of x-ray exposure parameters to the individual x-ray absorption profile of the patient, and prioritization of lower x-ray tube potentials in combination have resulted in dramatic reductions in patient radiation dose from thoracic CT. The introduction of iterative reconstruction algorithms has resulted in unprecedented reductions in radiation dose with preservation of diagnostic image quality. However, the fundamentals of good clinical practice such as the use of appropriateness criteria and correct patient positioning remain essential to maintaining radiation doses as low as reasonably achievable.

References

Beister M, Kolditz D, Kalender WA (2012) Iterative reconstruction methods in X-ray CT. Phys Med 28:94–108

Bendaoud S, Remy-Jardin M, Wallaert B et al (2011) Sequential versus volumetric computed tomography in the follow-up of chronic bronchopulmonary diseases: comparison of diagnostic information and radiation dose in 63 adults. J Thorac Imaging 26(3):190–195

Brenner DJ, Hall EJ (2007) Computed tomography- an increasing source of radiation exposure. N Engl J Med 357:2277–2284

Di Cesare E, Gennarelli A, Di Sibio A et al (2014) Assessment of dose exposure and image quality in coronary angiography performed by 640-slice CT: a comparison between adaptive iterative and filtered back-projection algorithm by propensity analysis. Radiol Med 2014(119):642–649

Dournes G, Verdier D, Montaudon M, Bullier E et al (2014) Dual-energy CT perfusion and angiography in chronic thromboembolic pulmonary hypertension: diagnostic accuracy and concordance with radionuclide scintigraphy. Eur Radiol 24(1):42–51

Einstein AJ, Moser KW, Thompson RC et al (2007) Radiation dose to patients from cardiac diagnostic imaging. Circulation 116:1290–1305

Fanous R, Kashani H, Jiménez L, Murphy G, Paul NS (2012) Image quality and radiation dose of pulmonary CT angiography performed using 100 and 120 kVp. AJR Am J Roentgenol 199(5):990–996

Fuchs TOJ et al (2000) Direct comparison of a xenon and a solid-state CT detector system: measurements under working conditions. IEEE Trans Med Imaging 19(9):941–948

Fujimoto S, Matsutani H, Kondo T et al (2013) Image quality and radiation dose stratified by patient heart rate for coronary 64- and 320-MDCT angiography. Am J Roentgenol 200(4):765–770

Godoy M, Naidich D, Marchiori E, Assadourian B et al (2009) Basic principles and postprocessing techniques of dual-energy CT: illustrated by selected congenital abnormalities of the thorax. J Thoracic Imag 24(2):152–159

Gosling O, Loader R, Venables P et al (2010) A comparison of radiation doses between state-of-the-art multislice CT coronary angiography with iterative reconstruction, multislice CT coronary angiography with standard filtered back-projection and invasive diagnostic coronary angiography. Heart 96:922–926

Hanna WC, Paul NS, Darling GE, Moshonov H, Allison F, Waddell TK, Cypel M, de Perrot ME, Yasufuku K, Keshavjee S, Pierre AF (2014) Minimal-dose computed tomography is superior to chest x-ray for the follow-up and treatment of patients with resected lung cancer. J Thorac Cardiovasc Surg 147(1):30

Hricak H, Brenner DJ, Adelstein SJ, Frush DP, Hall EJ et al (2011) Managing radiation use in medical imaging: a multifaceted challenge. Radiology 258(3):889–905

Idky EY, Kao CM, Pan X (2006) Accurate image reconstruction from few-views and limited-angle data in divergent-beam CT. J Sci Tech 14(2):119–139

Kalra M, Rizzo S, Maher M, Halpern E et al (2005) Chest CT performed with Z-axis modulation: scanning protocol and radiation dose. Radiology 237(1):303–308

Kaza RK, Platt JF, Cohan RH, Caoili EM, AlHawary MM, Wasnik A (2012) Dual-energy CT with single- and dual-source scanners: current applications in evaluating the genitourinary tract. Radio Graph 32:353–369

Ko JP, Brandman S, Stember J, Naidich DP (2012) Dual energy computed tomography: concepts, performance, and thoracic applications. J Thorac Imaging 27:7–22

Leipsic J, Labounty TM, Heilbron B et al (2010) Estimated radiation dose reduction using adaptive statistical iterative reconstruction in coronary CT angiography: the ERASIR study. AJR Am J Roentgenol 195(3):655–660

Murakami Y, Kakeda S, Kamada K, Ohnari N, Nishimura J, Ogawa M, Otsubo K, Morishita Y, Korogi Y (2010) Effect of tube voltage on image quality in 64-section multidetector 3D CT angiography: evaluation with a vascular phantom with superimposed bone skull structures. AJNR Am J Neuroradiol 31(4):620–625

Nakayama Y, Awai K, Funama Y, Hatemura M, Imuta M, Nakaura T, Ryu D, Morishita S, Sultana S, Sato N, Yamashita Y (2005) Abdominal CT with low tube voltage: preliminary observations about radiation dose, contrast enhancement, image quality, and noise. Radiology 237(3):945–951

Newton TD, Mehrez H, Wong K, Menezes R, Wintersperger BJ, Crean A, Nguyen E, Paul N (2011) Radiation dose threshold for coronary artery calcium score with MDCT: how low can you go? Eur Radiol 21(10):2121–2129

Odedra D, Blobel J, Alhumayyd S et al (2014) Image noise-based dose adaptation in dynamic volume CT of the heart: dose and image quality optimisation in comparison with BMI-based dose adaptation. Eur Radiol 24(1):86–94

Paul NS, Kashani H, Odedra D, Ursani A, Ray C, Rogalla P (2011) The influence of chest wall tissue composition in determining image noise during cardiac CT. AJR Am J Roentgenol 197(6):1328–1334

Pontana F, Faivre JB, Remy-Jardin M, Flohr T et al (2008) Lung perfusion with dual-energy multidetector-row CT (MDCT): feasibility for the evaluation of acute pulmonary embolism in 117 consecutive patients. Acad Radiol 15(12):1494–1504

Rogalla P, Blobel J, Kandel S, Meyer H, Mews J, Kloeters C, Kashani H, Lembcke A, Paul N (2010) Radiation dose optimisation in dynamic volume CT of the heart: tube current adaptation based on anterior-posterior chest diameter. Int J Cardiovasc Imaging 26(8):933–940

Schiham A, Molen AJ, Prokop M, de Jong HW (2010) Overranging at multisection CT: an underestimated source of excess radiation exposure. Radiographics 30(4):1057–1067

Spears JR, Schoepf UJ, Henzler T et al (2014) Comparison of the effect of iterative reconstruction versus filtered back projection on cardiac CT postprocessing. Acad Radiol 21(3):318–324

Wang R, Schoepf UJ, Wu R et al (2014) Diagnostic accuracy of coronary CT angiography: comparison of filtered back projection and iterative reconstruction with different strengths. J Comput Assist Tomogr 38(2):179–184

Wells PS, Ginsberg JS, Anderson DR et al (1998) Use of a clinical model for safe management of patients with suspected pulmonary embolism. Ann Intern Med 129:997–1005

Wells PS, Anderson DR, Rodger M et al (2001) Excluding pulmonary embolism at the bedside without diagnostic imaging: management of patients with suspected pulmonary embolism presenting to the emergency department by using a simple clinical model and d-dimer. Ann Intern Med 135:98–107

Williams MC, Weir NW, Mirsadraee S et al (2013) Iterative reconstruction and individualized automatic tube current selection reduce radiation dose while maintaining image quality in 320-multidetector computed tomography coronary angiography. Clin Radiol 68(11):e570–e577

Yuki H, Utsunomiya D, Funama Y et al (2014) Value of knowledge-based iterative model reconstruction in low-kV 256-slice coronary CT angiography. J Cardiovasc Comput Tomo 8(2):115–123